RESEARCH

Nonlinear analysis of the synchronous reference frame phase-locked loop under unbalanced grid voltage

Anton Ponomarev · Veit Hagenmeyer · Lutz Gröll

Abstract The synchronous reference frame phase-locked loop (SRF-PLL), also called dqPLL, is an electric circuit commonly used in power electronics to estimate the phase angle of a three-phase AC grid. If the voltage is unbalanced, the PLL is modeled as a periodically forced nonlinear oscillator and is known in practice to converge to a steady oscillation. In the existing literature, the oscillation has been studied via linearization assuming a low level of unbalance. Aiming for stronger nonlocal statements, we present nonlinear analysis. We apply the method of autonomous comparison systems and incremental stability to show that the steady oscillation is unique and attractive in a wider neighborhood. Its lock-in domain is estimated using numerical phase portrait analysis. The oscillation is further approximated up to the terms of the second order in the unbalance factor—it yields an estimation of the time average of the PLL's phase error which is not visible by linearization only. The results provide stability guarantees and can guide the tuning of SRF-PLL.

1 Introduction

Phase-locked loops (PLLs) are a class of dynamical systems designed to synchronize to the phase of a periodic signal. The synchronization problem arises in signal processing [5], sensing [16], power electronics [1], and other fields. We focus on a class of PLLs used in power electronics. They are an important component of many power inverters – notably, the grid-tied ones operating on the interface between a DC power source and the AC utility grid. The purpose of the PLL is to determine the phase of the AC grid voltage. The phase knowledge is then utilized to efficiently inject DC power into the AC grid [22].

We investigate a common PLL design called *synchronous reference frame PLL (SRF-PLL)* or *dqPLL* [7]. It is based on Park's *dq* coordinate transformation which transforms the voltage to a rotating reference frame. SRF-PLL achieves exact phase estimation only under balanced conditions – that is, when voltage amplitudes on all three wires are equal, and the phase angle differences between them are 120°. In reality,

A. Ponomarev, V. Hagenmeyer, and L. Gröll have contributed equally to this work.

A. Ponomarev (✉) · V. Hagenmeyer · L. Gröll
Institute for Automation and Applied Informatics, Karlsruhe Institute of Technology, Hermann-von-Helmholtz-Platz 1, 76344 Eggenstein-Leopoldshafen, Baden-Württemberg, Germany
e-mail: anton.ponomarev@kit.edu

V. Hagenmeyer
e-mail: veit.hagenmeyer@kit.edu

L. Gröll
e-mail: lutz.groell@kit.edu

grid voltage is always unbalanced. In this case, SRF-PLL phase estimation is contaminated by even harmonics of the grid's frequency – this is known from the experimental studies of PLLs under distorted voltage conditions [1].

In the previous literature, one finds two approaches to the analysis of the unbalance-induced oscillation. One method utilizes linearization, also known as the small angle approximation [7]. Another technique operates in the nonlinear setting and relies on a structural stability argument [6, Lemma 8]. Both of these approaches assume infinitesimal unbalance and yield small-angle results.

For large angles, SRF-PLL stability has been proven only under balanced conditions using the Lyapunov function method [9]. Extension of the nonlinear analysis to the unbalanced case is not easy for the reason that the nonlinear PLL equations affected by voltage unbalance are similar to those of a periodically forced nonlinear pendulum. It is well known that such equations may exhibit rich dynamics, including chaos [8]. This complicates the global stability analysis – with arbitrary angles and extra high unbalance. In this light, we aim for *regional* results (not so far from zero, but not infinitesimal either).

Our goal is to show that the oscillation observed in experiment is, in some sense, the only behavior practically possible. Specifically, we want to show that there is a "not small" region (the so-called *lock-in domain*) in which the oscillation is unique and attractive. We aim to estimate the lock-in domain better than is possible with the linearization or Lyapunov function methods. Furthermore, we are interested in approximating the time average of the oscillation. Our motivation is explained more substantially in Sect. 2.5, and the goals are formulated in Sect. 2.6. The main analytical results are described in Sect. 4.1, their numerical application is illustrated in Sect. 4.2.

2 Preliminaries

2.1 SRF-PLL dynamics

Let us introduce the equations governing the SRF-PLL circuit in an unbalanced AC grid with frequency ω:

$$\dot{\delta} = -K_1 \mu(2\omega t) \sin \delta + \gamma + \omega F(\mu(2\omega t)), \quad (1a)$$

$$\dot{\gamma} = -K_2 \mu(2\omega t) \sin \delta \quad (1b)$$

where

$$F(\mu) = 1 - \frac{1 - \kappa^2}{\mu^2}. \quad (1c)$$

These equations are derived in Appendix A (Proposition 3). The terms have the following meaning:

- δ is the dynamical part of the phase estimation error produced by the PLL;
- γ is the frequency estimation error;
- $K_1 > 0$ and $K_2 > 0$ are constants that depend on the parameters of the voltage (magnitude and frequency) and parameters of the internal control loop within PLL – these constants can be tuned by the engineer;
- $\kappa \in [0, 1)$ is a constant called the *unbalance factor* – larger κ corresponds to stronger unbalance;
- $\mu(\cdot)$ is the 2π-periodic unbalance-induced forcing function

$$\mu(\psi) = \sqrt{1 + 2\kappa \cos \psi + \kappa^2} \quad (2)$$

which satisfies the bounds

$$0 < 1 - \kappa \le \mu(\cdot) \le 1 + \kappa. \quad (3)$$

Remark 1 System (1) presumes several *modeling assumptions*: grid voltage conditions are time-invariant; the voltage sensor is ideal; the PLL is implemented as an analog circuit or at a very high sampling rate; the dq transformation (a signal multiplier inside the PLL which plays the role of a phase detector) is based on the ideal sine waveform.

Remark 2 System (1) is similar to the equations of a *single*-phase PLL [18, Eq. (5)]. The main difference, introduced by the voltage unbalance, is the fact that our system (1) is time-varying despite constant voltage conditions.

System (1) is symmetric with respect to 2π-shifts in δ, so we consider the PLL in the *cylindrical phase space* $\mathbb{S}^1 \times \mathbb{R}$ where points (δ, γ) and $(\delta + 2\pi, \gamma)$ are identical.

Formally, system (1) is a nonlinear oscillator where function $\mu(\cdot)$ governs both the forcing term and parametric excitation. Unbalance factor κ is a parameter that quantifies the magnitude of $\mu(\cdot)$.

2.2 Normalized equations

Observe that the constants K_1 and K_2 in (1) are influenced by the designer of the PLL, whereas the main grid

frequency ω and the unbalance-induced function $\mu(\cdot)$ are uncontrollable factors. In order to limit our analysis to only one unknown, we eliminate ω via normalization in the following way:

- use normalized timescale $\tau = \omega t$;
- introduce new system variables: dynamical phase error $\beta(\tau) = \delta(t)$ and *relative* frequency error $\zeta(\tau) = \gamma(t)/\omega$;
- define coefficients $C_1 = K_1/\omega$, $C_2 = K_2/\omega^2$.

With these modifications, the PLL system (1) changes to

$$\beta' = -C_1\mu(2\tau)\sin\beta + \zeta + F(\mu(2\tau)), \qquad (4a)$$
$$\zeta' = -C_2\mu(2\tau)\sin\beta \qquad (4b)$$

where the prime $\ldots'$ means differentiation with respect to τ.

Note that coefficients C_1 and C_2 are related to the parameters K_p and K_i of the PI controller within the PLL: due to (A18c) we have

$$C_1 = \frac{K_p|\Phi_p|}{\omega}, \quad C_2 = \frac{K_i|\Phi_p|}{\omega^2} \qquad (5)$$

where $|\Phi_p|$ is the positive sequence voltage amplitude and ω is the voltage frequency. Therefore, C_1 and C_2 can be interpreted as tunable parameters.

From now on, we consider the normalized PLL dynamics (4) on the cylinder $\mathbb{S}^1 \times \mathbb{R}$.

2.3 Basic notions in the balanced case

In the balanced case we have $\kappa = 0$ and $\mu(\cdot) \equiv 1$, so system (4) reduces to

$$\beta' = -C_1\sin\beta + \zeta, \qquad (6a)$$
$$\zeta' = -C_2\sin\beta. \qquad (6b)$$

In $\mathbb{S}^1 \times \mathbb{R}$, the system has a stable equilibrium ($\beta = \zeta = 0$) and a saddle point ($\beta = \pm\pi$, $\zeta = 0$).

Using the variable $x = \beta - \frac{C_1}{C_2}\zeta$ system (6) is equivalent to one equation $x'' + C_2 \sin\left(\frac{C_1}{C_2}x' + x\right) = 0$ which is similar to a nonlinear pendulum $x'' + C_1 x' + C_2 \sin x = 0$. Following the pendulum analogy, the "energy" function $E = 1 - \cos\beta + \frac{1}{2C_2}\zeta^2$ decreases along the trajectories of (6) except at the points where $\sin\beta = 0$ since $E' = -C_1 \sin^2\beta \leq 0$. A modification of LaSalle's

invariance principle [20, Theorem 4.2.1] proves that every trajectory converges to an equilibrium. Obviously, almost all trajectories converge to the stable equilibrium $(0, 0)$. The only exception is the stable separatrices approaching the saddle $(\pm\pi, 0)$.

More detailed discussion of SRF-PLL stability in the balanced case can be found in [9].

It will be convenient to distinguish two cases based on the quality of the linearization at the stable equilibrium: the oscillatory case and the overdamped case. In the oscillatory case, the stable equilibrium is a focus; otherwise, it is a node. The two cases are illustrated by Fig. 1. Which case is present depends on the *quality factor* (*Q factor*)

$$Q = \sqrt{\frac{C_2}{C_1^2}}. \qquad (7)$$

With $Q > 1/2$ the balanced PLL is oscillatory, and for $Q < 1/2$ it is overdamped.

The initial points can be classified depending on the number of times n that the corresponding trajectory crosses the line $\beta = \pm\pi$. If $n = 0$, PLL converges to the closest equilibrium $(0, 0)$. If $n \neq 0$, PLL goes around the phase cylinder and eventually settles at one of the aliases of $(0, 0)$: either $(2n\pi, 0)$ or $(-2n\pi, 0)$. The behavior with $n \neq 0$ may be called *cycle slipping*.

Remark 3 Several variations of the notion of *cycle slipping* are established in the theory of single-phase PLLs [19, Definitions 4, 4′]. Our interpretation of this concept is still slightly different. According to [19], there is no cycle slipping if $|\beta(0) - \beta(t)| \leq 2\pi$, either in the upper limit as $t \to \infty$ or at every t. We, on the other hand, say that there is no cycle slipping if $\beta(t)$ never crosses the line $\beta = \pm\pi$. *Our condition is stronger*: assuming $|\beta(0)| \leq \pi$, it implies $|\beta(t)| \leq \pi$ for all t and therefore guarantees that there is no cycle slipping in the sense of [19] either. Our definition of cycle slipping via crossings with the line $\beta = \pm\pi$ is motivated by the fact that the line is an invariant reference object. As for the definitions from [19], they are formulated in reference to the arbitrary initial point $\beta(0)$ or to the limit set of $\beta(t)$ – this proves to be less convenient in our case.

The initial points that do not produce cycle slipping are said to belong to the *lock-in domain* [19]. The lock-in domain of the balanced PLL (6) is shown in Fig. 1
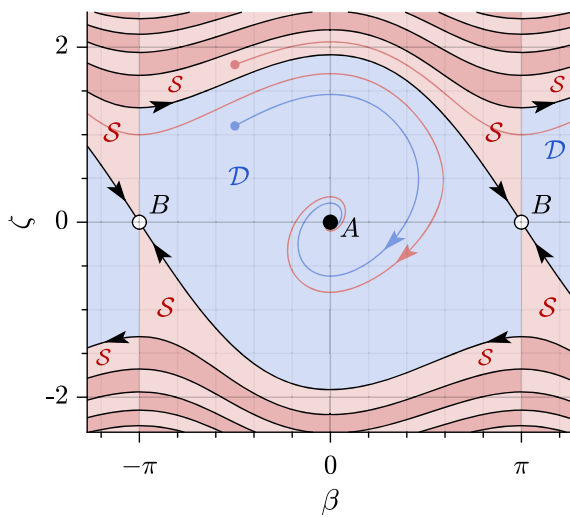
(a) Oscillatory case.
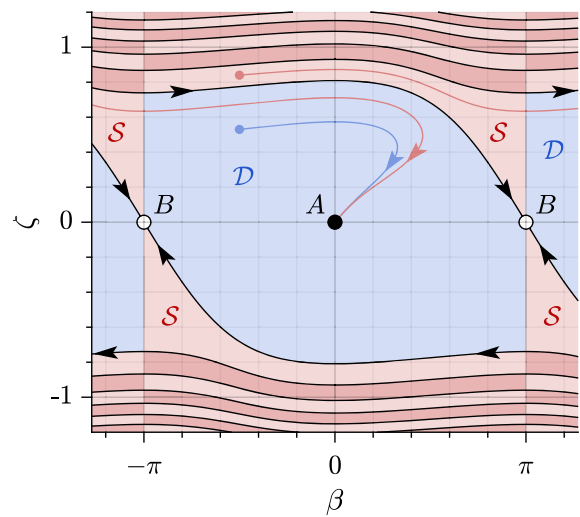
(b) Overdamped case.

Fig. 1 Behavior of the balanced PLL (6). A – stable equilibrium. B – saddle point. Black lines – stable separatrices approaching B. Blue region $\mathcal{D}$ – lock-in domain. Trajectories starting in the

red region $\mathcal{S}$ make one crossing with the line $\beta = \pm\pi$. For other red regions, there are two, three, and more crossings

as the blue region $\mathcal{D}$. The set of initial points leading to one crossing with $\beta = \pm\pi$ is the red region $\mathcal{S}$.

2.4 Basic notions for the unbalanced case

Balanced PLL (6) has constants C_1 and C_2 where the unbalanced PLL (4) has periodic parameters $C_1\mu(2\tau)$ and $C_2\mu(2\tau)$. For our purposes, we formally extend the definition of the quality factor (7) to the unbalanced case via replacing C_1 and C_2 by their time-varying counterparts. This leads to the time-varying quality factor

$$Q(\tau) = \sqrt{\frac{C_2}{C_1^2\mu(2\tau)}} \tag{8}$$

and the following definition.

Definition 1 PLL (4) under given voltage conditions is called *oscillatory* if $Q(\tau) > 1/2$ for all τ. It is called *overdamped* if $Q(\tau) < 1/2$ for all τ.

The type of a PLL depends on the voltage conditions since the range (3) of $\mu(\cdot)$ is affected by the voltage unbalance. Moreover, coefficients C_1 and C_2 from (5) are influenced by the voltage parameters as well as by

the tuning of the PLL. If voltage parameters are within specified operating limits, the ratio C_2/C_1^2 in (8) can be robustly tuned so that $Q(\tau)$ is always on the same side of $1/2$.

Remark 4 We do not discuss the intermediate case where $Q(\tau)$ goes above and below $1/2$ over the course of time, but this case can be treated similarly to our approach.

In this paper we are interested in the periodic solutions of (4) – the so-called steady oscillations.

Definition 2 A *steady oscillation* is a periodic solution of the PLL (4).

The balanced-case definition of the lock-in domain as the domain of "immediate" convergence to the stable equilibrium is trivially extended to the unbalanced case as follows. Note that due to the time-variability of (4) we need to mention the initial time in this definition.

Definition 3 The *lock-in domain* is the set of initial states (β_0, ζ_0) from which the PLL (4) converges to a steady oscillation near $(0, 0)$ without crossing the line $\beta = \pm\pi$, independently of the initial time t_0 at which the state (β_0, ζ_0) occurs.

2.5 Practical motivation

Consider a power inverter that injects electrical power from a DC source into the AC grid. The inverter uses a PLL circuit to estimate the instantaneous phase angle of the grid voltage. Ideally, power should be injected in-phase with the grid to minimize losses. The larger the phase error of the PLL, the less efficient the inverter's operation. In addition, if the PLL error is persistently oscillating, the inverter will translate this oscillation into the grid, thus compromising the voltage waveform. This explains why it is useful to understand the PLL's phase error.

Let us discuss the physical meaning of the lock-in domain. Suppose the PLL is in a steady state when the operating conditions change suddenly – for example, due to a change in the voltage conditions or at the startup of the PLL. If the PLL state is in the post-change lock-in domain, the phase error goes into the steady oscillation directly, without making unnecessary turns around the phase cylinder. Such behavior is predictable and clearly desirable in practice.

As a final thought, suppose that one wants to average the phase error oscillation over time in order to simplify the overall system analysis. The time average of the phase error is important because non-zero phase error translates to a non-zero time delay which may have interesting consequences. Nonlinear analysis is necessary to capture the average phase error since it turns out to be a term of order κ^2.

2.6 Goals of the study

Based on the practical considerations from the previous section, we set the following goals:

1. To localize a unique steady oscillation $\mathcal{O}_1$ of the PLL near the origin $(0, 0)$.
2. To construct an *inner* approximation of the lock-in domain.
3. To construct an *outer* approximation of the lock-in domain.
4. To approximate the time average of the dynamical phase error β during the oscillation $\mathcal{O}_1$.

Remark 5 These goals are concerned with the characteristics of the system that do not depend on the timescale. Thus, results we obtain for the normalized system (4) are valid for the original model (1) as well.

3 Auxiliary results

3.1 Autonomous comparison systems

Our analysis is based on the concept of *autonomous comparison systems*. These are time-invariant systems whose trajectories can be used to estimate the trajectories of a time-varying system such as (4). The approach has been described in [4] for the second-order systems in the standard form

$$\dot{x} = y, \tag{9a}$$
$$\dot{y} = Y(x, y, t). \tag{9b}$$

For our purposes, it is more convenient to consider the PLL equations in their original form (4). We adapt the technique of [4] for second-order systems

$$\dot{x} = X(x, y, t), \tag{10a}$$
$$\dot{y} = Y(x, y, t) \tag{10b}$$

in the following way. Suppose that there exist time-invariant vector fields $(X_{\text{left}}, Y_{\text{left}})$ and $(X_{\text{right}}, Y_{\text{right}})$ such that for all $(x, y) \in \mathbb{R}^2$

$$\inf_t \left\langle \begin{bmatrix} X(x, y, t) \\ Y(x, y, t) \end{bmatrix}, \begin{bmatrix} Y_{\text{left}}(x, y) \\ -X_{\text{left}}(x, y) \end{bmatrix} \right\rangle = 0 \tag{11a}$$

and

$$\sup_t \left\langle \begin{bmatrix} X(x, y, t) \\ Y(x, y, t) \end{bmatrix}, \begin{bmatrix} Y_{\text{right}}(x, y) \\ -X_{\text{right}}(x, y) \end{bmatrix} \right\rangle = 0 \tag{11b}$$

where $\langle \cdot, \cdot \rangle$ is the dot product.

Definition 4 The systems

$$\dot{x} = X_{\text{left}}(x, y), \tag{12a}$$
$$\dot{y} = Y_{\text{left}}(x, y) \tag{12b}$$

and

$$\dot{x} = X_{\text{right}}(x, y), \tag{13a}$$
$$\dot{y} = Y_{\text{right}}(x, y) \tag{13b}$$

defined by (11) are called, respectively, the *left* and *right autonomous comparison systems* for (10).

Remark 6 We use the descriptors "left" and "right" in the standard sense: given planar vectors v, v_{left}, and
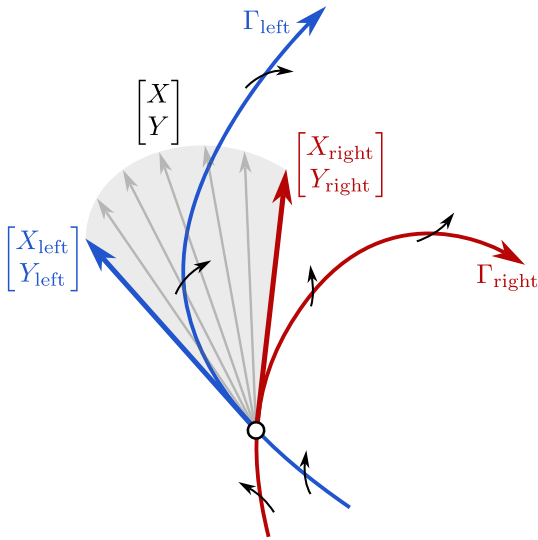
Fig. 2 Illustration of the idea behind Definition 4. Γ_{left} and Γ_{right} are trajectories of the comparison systems (12) and (13). Small arrows represent possible directions in which the trajectories of the time-varying system (10) can cross Γ_{left} and Γ_{right}

v_{right}, we say that v_{left} is to the left of v, and v_{right} is to the right of v if the shortest rotation from v to v_{left} is counterclockwise, and from v to v_{right} clockwise.

Definition 4 is illustrated by Fig. 2. It shows the cone of possible directions (X, Y) that the original time-varying system (10) can move in at the given point. The leftmost direction in this cone is $(X_{\text{left}}, Y_{\text{left}})$, and the rightmost direction is $(X_{\text{right}}, Y_{\text{right}})$. The following statement is a useful direct implication of Definition 4.

Proposition 1 *If the left comparison system* (12) *has a limit cycle orbiting clockwise then the area within the limit cycle is a forward invariant set of* (10).

Proof Suppose Γ_{left} is a trajectory of the left comparison system. It follows from Definition 4 that solutions of (10) can only cross Γ_{left} rightward, relative to the direction of Γ_{left} – this is shown by small arrows in Fig. 2. In particular, if Γ_{left} is a clockwise limit cycle, then it is crossed by (10) inward. Therefore, the interior of Γ_{left} is a forward invariant set of (10). $\qquad\square$

Remark 7 The geometric interpretation of the comparison systems assumes that they have unique smooth solutions. This implicit assumption will hold in our analysis.

The following lemma suggests a simplified way of computing the comparison dynamics for a class of systems which covers our PLL dynamics (4).

Lemma 1 *For the system*

$$\dot{x} = f(t)X(x, y, t), \tag{14a}$$
$$\dot{y} = f(t)Y(x, y) \tag{14b}$$

where $f(\cdot) \geq \text{const} > 0$ *the comparison systems* (12) *and* (13) *are formed by*

$$Y_{\text{left}}(x, y) = Y_{\text{right}}(x, y) = Y(x, y) \tag{15a}$$

and

$$X_{\text{left}}(x, y) = \begin{cases} \inf_t X(x, y, t), & Y(x, y) \geq 0, \\ \sup_t X(x, y, t), & Y(x, y) < 0, \end{cases} \tag{15b}$$

$$X_{\text{right}}(x, y) = \begin{cases} \sup_t X(x, y, t), & Y(x, y) \geq 0, \\ \inf_t X(x, y, t), & Y(x, y) < 0. \end{cases} \tag{15c}$$

Proof By a change of the time variable, factor $f(t)$ is eliminated from the system equations. This does not change the system's orbits and, therefore, does not affect the comparison systems. The statement (15) then follows from (11). $\qquad\square$

Application of Lemma 1 gives the following explicit form of the comparison systems for (4).

Corollary 1 *The left comparison system for the PLL* (4) *is*

$$\beta' = -C_1 \sin\beta + G\big(\text{sign}(\sin\beta), \zeta\big), \tag{16a}$$
$$\zeta' = -C_2 \sin\beta \tag{16b}$$

and the right one is

$$\beta' = -C_1 \sin\beta + G\big(-\text{sign}(\sin\beta), \zeta\big), \tag{17a}$$
$$\zeta' = -C_2 \sin\beta \tag{17b}$$

where

$$G(-1, \zeta) = \min_\mu \frac{\zeta + F(\mu)}{\mu}$$
$$= \min\left\{ \frac{\zeta - \zeta_-}{1 + \kappa}, \frac{\zeta - \zeta_+}{1 - \kappa} \right\}, \tag{18a}$$

$$G(+1, \zeta) = \max_{\mu} \frac{\zeta + F(\mu)}{\mu}$$

$$= \begin{cases} \dfrac{\zeta - \zeta_+}{1 - \kappa}, & \zeta \geq 2 \cdot \dfrac{1 + 2\kappa}{1 - \kappa}, \\ \dfrac{\zeta - \zeta_-}{1 + \kappa}, & \zeta < 2 \cdot \dfrac{1 - 2\kappa}{1 + \kappa}, \\ \dfrac{2}{3} \sqrt{\dfrac{(\zeta + 1)^3}{3(1 - \kappa^2)}}, & \text{otherwise} \end{cases}$$

$$(18b)$$

with

$$\zeta_+ = \frac{2\kappa}{1 - \kappa}, \quad \zeta_- = -\frac{2\kappa}{1 + \kappa}. \tag{18c}$$

The value of $G(0, \zeta)$ can be set equal to $G(-1, \zeta)$ or $G(+1, \zeta)$ arbitrarily – it will not affect the solutions of the comparison systems when they exist.

Proof The statement follows from Lemma 1 after straightforward calculations. □

The functions $G(\pm 1, \zeta)$ are, respectively, the upper and lower bounds on $(\zeta + F(\mu))/\mu$:

$$G(-1, \zeta) \leq \frac{\zeta + F(\mu)}{\mu} \leq G(+1, \zeta) \tag{19}$$

for all $\mu \in [1 - \kappa, 1 + \kappa]$. Together with the fact

$$G(-1, \zeta_+) = G(+1, \zeta_-) = 0 \tag{20}$$

it implies that in (4)

$$\beta' > 0 \text{ when } \beta = 0 \text{ and } \zeta > \zeta_+, \tag{21a}$$
$$\beta' < 0 \text{ when } \beta = 0 \text{ and } \zeta < \zeta_-. \tag{21b}$$

This observation together with Corollary 1 will be instrumental in the proof of Theorem 1 below and in the numerical estimations of Sect. 4.2.

3.2 Stability of a time-varying linear equation

The following lemma gives a sufficient condition for the stability of a linear time-varying second-order equation. It will be applied in the proof of Theorem 1 to establish linearization-based incremental asymptotic stability of (4) in a neighborhood of the origin – that is, convergence of any two of its solutions to each other [3, Definition 3.3].

Lemma 2 *Equation*

$$m(t)\ddot{x} + k\dot{x} + x = 0 \tag{22}$$

with $0 < m_{\min} \leq m(t) \leq m_{\max} < \infty$ is uniformly exponentially stable if

$$k > \sqrt{m_{\max}} - \sqrt{m_{\min}}. \tag{23}$$

Proof Consider the quadratic Lyapunov function candidate

$$v(x, \dot{x}) = \begin{bmatrix} x & \dot{x} \end{bmatrix} P \begin{bmatrix} x \\ \dot{x} \end{bmatrix} \quad \text{with} \quad P = \begin{bmatrix} 1 & a \\ a & b \end{bmatrix} \tag{24}$$

whose derivative along the solutions of (22) is

$$\dot{v}\big|_{(22)} = -\begin{bmatrix} x & \dot{x} \end{bmatrix} R \begin{bmatrix} x \\ \dot{x} \end{bmatrix} \tag{25a}$$

with

$$R = \frac{1}{m(t)} \begin{bmatrix} 2a & ka + b - m(t) \\ ka + b - m(t) & 2(kb - am(t)) \end{bmatrix}. \tag{25b}$$

System (22) is uniformly exponentially stable if P and R are positive definite uniformly in t. This holds if

$$a > 0, \tag{26a}$$
$$a^2 - b < 0, \tag{26b}$$
$$p(m; a, b) < 0 \quad \text{for all } m \in [m_{\min}, m_{\max}] \tag{26c}$$

where $p(m; a, b) = m^2 - 2(ka + b - 2a^2)m + (ka - b)^2$. Suppose $m = m_1$ and $m = m_2$ are the roots of p. Inequality (26c) is satisfied if and only if

$$0 < m_1 < m_{\min} < m_{\max} < m_2. \tag{27}$$

We are going to show that under the conditions of the lemma there exist m_1 and m_2 that satisfy (27) and correspond to the values of a and b that satisfy (26a) and (26b).

From Vieta's formulas

$$\frac{m_1 + m_2}{2} = ka + b - 2a^2, \tag{28a}$$
$$\pm\sqrt{m_1 m_2} = ka - b \tag{28b}$$

which yields

$$2(a^2 - b) = \pm\sqrt{m_1 m_2} - \frac{m_1 + m_2}{2} < 0 \qquad (29)$$

due to the inequality of the algebraic and geometric means. This shows that (26b) already follows from (27). Moreover, from (28)

$$2(a^2 - ka) = \mp\sqrt{m_1 m_2} - \frac{m_1 + m_2}{2}. \qquad (30)$$

For (26a) to be satisfied, (30) should have a positive root a which implies

$$\mp\sqrt{m_1 m_2} - \frac{m_1 + m_2}{2} > -\frac{k^2}{2} \qquad (31)$$

for at least one of the signs: "+" or "−". We can assume the "+" sign and thus require

$$m_1 - 2\sqrt{m_1 m_2} + m_2 < k^2 \qquad (32)$$

which is equivalent to

$$\sqrt{m_2} - \sqrt{m_1} < k. \qquad (33)$$

Existence of m_1 and m_2 that satisfy (27) and (33) follows from the conditions of the lemma. □

Remark 8 What we have just proven in Lemma 2 is actually *quadratic stability*, i.e., existence of a quadratic Lyapunov function. This concept, common in the area of uncertain systems, is stronger than general asymptotic stability [2, Chapter 3]. Although conservative, such a result is sufficient for our purposes.

4 Main results

4.1 Analytical statements

Our first main theorem establishes the existence of a unique locally attractive oscillation near the origin for small values of unbalance. Its proof demonstrates the use of a left comparison system. In the context of PLL analysis, an important limitation of the comparison systems approach is the fact that it always assumes a "worst case" of the function $\mu(\cdot)$. That is, the shape of the actual function $\mu(\cdot)$ given by (2) is not taken into account. Nevertheless, the proof of Theorem 1 is constructive. It lays the road to goals 1–3 from Sect. 2.6

enabled by the numerical simulation of the comparison systems. This is demonstrated in Sect. 4.2.1.

Theorem 1 (Existence of an attractive steady oscillation) *There exist a constant* $\kappa \in (0, 1)$ *and a set* $\mathcal{E} \subset \{(\beta, \zeta)\}$ *containing the origin such that for an arbitrary* 2π-*periodic piecewise continuous function* $\mu(\cdot) \in [1 - \kappa, 1 + \kappa]$ *the set* $\mathcal{E}$ *is forward invariant for* (4) *and contains at least one* π-*periodic steady oscillation. The diameter of* $\mathcal{E}$ *is* $O(\kappa)$ *as* $\kappa \to 0$. *Furthermore, if*

$$|\beta| < \arccos\left(\frac{\sqrt{\dfrac{C_2}{1 - \kappa}}}{C_1 + \sqrt{\dfrac{C_2}{1 + \kappa}}}\right)^2 \qquad (34)$$

for all $(\beta, \zeta) \in \mathcal{E}$ *then* $\mathcal{E}$ *contains exactly one steady oscillation which attracts all solutions of* (4) *starting in* $\mathcal{E}$.

Proof Our approach to the construction of $\mathcal{E}$ is shown in Fig. 3 in the oscillatory and overdamped cases as per Definition 1.

Let us discuss the *oscillatory case* first. Consider the balanced conditions ($\kappa = 0$) and pick a trajectory of the balanced PLL (6) that wraps around the origin. This is the black curve Γ on the left side of Fig. 3. That such a trajectory exists is clear from the structure of the balanced oscillatory phase portrait (see Fig. 1).

Next, consider unbalanced conditions: $\kappa > 0$. The trajectory of (4) starting from P_0 will generally deviate from Γ due to the influence of $\mu(\cdot)$. We apply the method of autonomous comparison systems to estimate the perturbed trajectory. The trajectory of the left comparison system (16) starting from P_0 is shown in Fig. 3 as the blue curve Γ'. The comparison system "tries to oscillate" around the focal point $A_-(0, \zeta_-)$ when $\sin\beta > 0$ and around $A_+(0, \zeta_+)$ when $\sin\beta < 0$. For small enough κ, point A_+ remains below P_1, and P_1' remains below P_0 by continuity. As the domain $\mathcal{E}$ we then choose the blue Bendixson pocket $\mathcal{E}$ bounded by Γ' and the segment $P_1'P_0$. The small arrows in Fig. 3 show the possible directions of the unbalanced PLL (4) on the boundary of $\mathcal{E}$. The vertical segment is crossed from left to right due to the property (21). The curve Γ' is always pierced inward by the fundamental property of comparison trajectories. Therefore, $\mathcal{E}$ is a forward invariant set of (4).
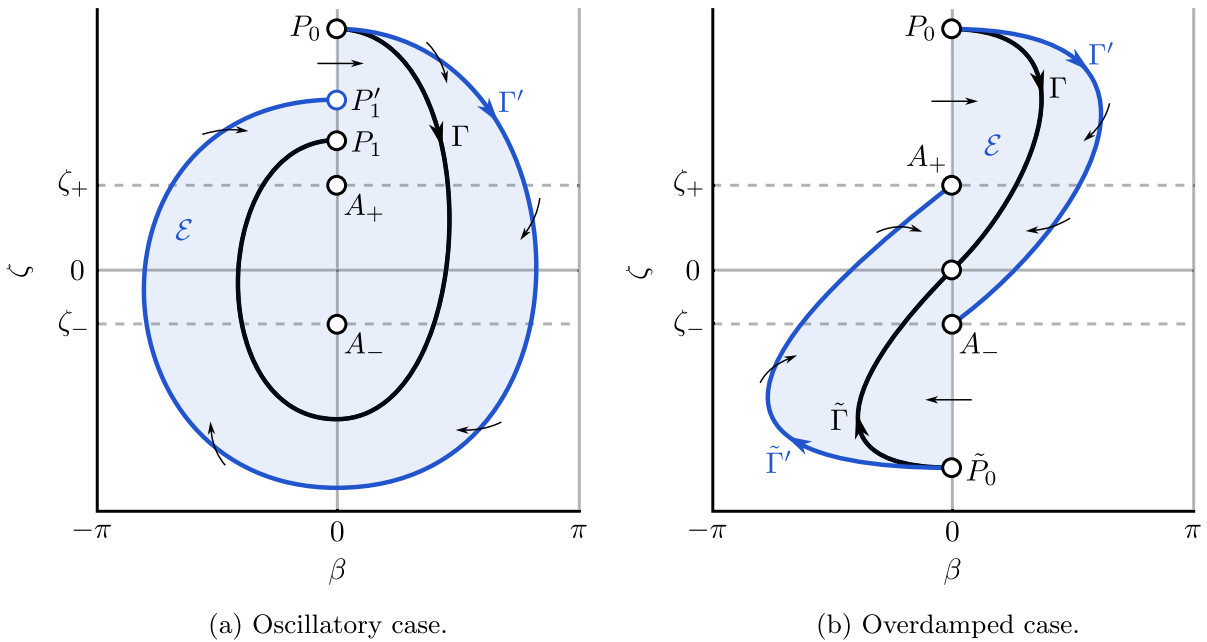
(a) Oscillatory case.

(b) Overdamped case.

Fig. 3 Illustration for the proof of Theorem 1. Γ, $\tilde{\Gamma}$ – trajectories of the balanced PLL (6). Γ', $\tilde{\Gamma}'$ – trajectories of the left comparison system (16). $\mathcal{E}$ – a forward invariant set of the unbalanced PLL (4). Small arrows – directions in which the trajectories of (4) may cross the boundary of $\mathcal{E}$

The *overdamped case* differs from the oscillatory one in that Γ approaches the origin without encircling it. To construct the domain $\mathcal{E}$, consider also another trajectory $\tilde{\Gamma}$ of the balanced PLL (6) that starts from a point $\tilde{P}_0$ on the negative ζ-axis. With small κ, the left comparison system (16) will have trajectories Γ' and $\tilde{\Gamma}'$ as in Fig. 3. Then $\mathcal{E}$ is bounded by Γ', $\tilde{\Gamma}'$, and the segments $A_+ P_0$ and $A_- \tilde{P}_0$. In all other aspects, the above discussion holds in the overdamped case as well.

With forward invariance of $\mathcal{E}$ established, it is only a matter of applying Brouwer's fixed-point theorem to the Poincaré map $\big(\beta(0), \zeta(0)\big) \mapsto \big(\beta(\pi), \zeta(\pi)\big)$ produced by (4) to assert that $\mathcal{E}$ contains at least one π-periodic steady oscillation [24, Theorem 15.1].

To show that the diameter of $\mathcal{E}$ is $O(\kappa)$, suppose that the ζ-coordinate of point P_0 in Fig. 3 is $\zeta_0 \approx 0$. In the oscillatory case it is easy to confirm, e.g., via a linearization argument, that $\zeta_0 = O(|P_0 P_1|)$ as $|P_0 P_1| \to 0$. Furthermore, $|P_1 P_1'| = O(\kappa)$ as $\kappa \to 0$. Then, by requiring, e.g., $|P_1 P_1'| = \frac{1}{2}|P_0 P_1|$ we set up a relation between ζ_0 and κ which implies $\zeta_0 = O(|P_0 P_1|) = O(|P_1 P_1'|) = O(\kappa)$. The diameter of $\mathcal{E}$ is therefore $O(\zeta_0) + O(\kappa) = O(\kappa)$. A similar argument can be made in the overdamped case too.

Assuming now that condition (34) holds, we show that all solutions of (4) located in $\mathcal{E}$ converge to each other. Consider two such solutions (β_1, ζ_1) and (β_2, ζ_2). We have

$$\triangle\beta' = -2C_1\mu(2\tau)\cos\frac{\beta_1 + \beta_2}{2}\sin\frac{\triangle\beta}{2} + \triangle\zeta, \quad (35a)$$

$$\triangle\zeta' = -2C_2\mu(2\tau)\cos\frac{\beta_1 + \beta_2}{2}\sin\frac{\triangle\beta}{2} \quad (35b)$$

where

$$\triangle\beta = \beta_1 - \beta_2, \quad \triangle\zeta = \zeta_1 - \zeta_2. \quad (36)$$

Using the variable

$$x = \triangle\beta - \frac{C_1}{C_2}\triangle\zeta \quad (37)$$

we obtain

$$x'' + 2g(\tau)\sin\frac{x + \dfrac{C_1}{C_2}x'}{2} = 0 \quad (38)$$

where

$$g(\tau) = C_2 \mu(2\tau) \cos \frac{\beta_1 + \beta_2}{2}. \tag{39}$$

Linearization of (38) about the zero solution is

$$\frac{1}{g(\tau)} x'' + \frac{C_1}{C_2} x' + x = 0. \tag{40}$$

Due to (34)

$$\frac{1}{C_2(1+\kappa)} \leq \frac{1}{g(\tau)} < \left(\frac{C_1}{C_2} + \sqrt{\frac{1}{C_2(1+\kappa)}} \right)^2 \tag{41}$$

for all τ, and Lemma 2 asserts asymptotic stability of the linearization (40). By virtue of the linearized stability principle this means that (4) is locally incrementally asymptotically stable inside $\mathcal{E}$ [11, Proposition 3.3]. That is, all solutions of (4) in $\mathcal{E}$ converge to each other and eventually to the steady oscillation which is therefore unique within $\mathcal{E}$. □

Our second theorem uses more information about the actual function $\mu(\cdot)$ given by (2) in order to attain goal 4 of Sect. 2.6. It provides an estimation of order κ^2 of the time average of β. The proof is based on the partial Taylor expansion of the steady oscillation established in Theorem 1.

Theorem 2 (Time average of the dynamical phase error) *Under the conditions of Theorem 1, including (34), the time average $\overline{\beta}$ of the dynamical phase error β corresponding to the steady oscillation from Theorem 1 can be expressed as*

$$\overline{\beta} = \overline{\beta}_2 \kappa^2 + O\left(\kappa^3\right) \tag{42a}$$

where

$$\overline{\beta}_2 = -\frac{4C_1}{4C_1^2 + (C_2 - 4)^2}. \tag{42b}$$

Proof We trivially obtain

$$\mu(\phi) = 1 + \kappa \cos \phi + O\left(\kappa^2\right), \tag{43a}$$

$$F\left(\mu(\phi)\right) = 2\kappa \cos \phi - 2\kappa^2 \cos 2\phi + O\left(\kappa^3\right) \tag{43b}$$

and search for a periodic solution of (4) as

$$\beta = \beta_1(\tau)\kappa + \beta_2(\tau)\kappa^2 + \beta_{3+}(\tau, \kappa), \tag{44a}$$

$$\zeta = \zeta_1(\tau)\kappa + \zeta_2(\tau)\kappa^2 + \zeta_{3+}(\tau, \kappa). \tag{44b}$$

Plugging these expressions together with (43) into (4) and balancing the coefficients before the powers of κ we find that the coefficients in the terms of order κ and κ^2 satisfy the linear equations

$$\frac{\mathrm{d}}{\mathrm{d}\tau} \begin{bmatrix} \beta_1 \\ \zeta_1 \end{bmatrix} = A \begin{bmatrix} \beta_1 \\ \zeta_1 \end{bmatrix} + \begin{bmatrix} 2\cos 2\tau \\ 0 \end{bmatrix}, \tag{45a}$$

$$\frac{\mathrm{d}}{\mathrm{d}\tau} \begin{bmatrix} \beta_2 \\ \zeta_2 \end{bmatrix} = A \begin{bmatrix} \beta_2 \\ \zeta_2 \end{bmatrix} - \begin{bmatrix} 2\cos 4\tau \\ 0 \end{bmatrix} - B\beta_1(\tau) \cos 2\tau \tag{45b}$$

where

$$A = \begin{bmatrix} -C_1 & 1 \\ -C_2 & 0 \end{bmatrix}, \quad B = \begin{bmatrix} C_1 \\ C_2 \end{bmatrix}. \tag{45c}$$

The equations have a unique periodic solution in the form

$$\beta_1 = \beta_1^{\cos} \cos 2\tau + \beta_1^{\sin} \sin 2\tau, \tag{46a}$$

$$\beta_2 = \overline{\beta}_2 + \beta_2^{\cos} \cos 4\tau + \beta_2^{\sin} \sin 4\tau \tag{46b}$$

with some constants $\beta_{1,2}^{\cos,\sin}$ and $\overline{\beta}_2$. Simple calculations confirm that the time average $\overline{\beta}_2$ is given by (42b).

To complete the proof, we need to show that the residual terms β_{3+} and ζ_{3+} are $O(\kappa^3)$. We have

$$\frac{\mathrm{d}}{\mathrm{d}\tau} \begin{bmatrix} \beta_{3+} \\ \zeta_{3+} \end{bmatrix} = A \begin{bmatrix} \beta_{3+} \\ \zeta_{3+} \end{bmatrix} + \boldsymbol{g}(\tau) \tag{47a}$$

where

$$\boldsymbol{g}(\tau) = B\mu(2\tau)(\beta - \sin \beta) + O\left(\kappa^3\right). \tag{47b}$$

Theorem 1 implies that the steady oscillation has diameter $O(\kappa)$ as $\kappa \to 0$. Therefore, $\beta = O(\kappa)$ and consequently $\boldsymbol{g} = O(\kappa^3)$. Furthermore, Lemma 2 due to (34) asserts that the linear part of the system (47) is uniformly exponentially stable. On these grounds we conclude that the unique periodic solution of (47) is indeed $O(\kappa^3)$. □

4.2 Numerical estimations

To demonstrate the application of our methods, let us consider SRF-PLL (4) in two cases: an *oscillatory case* with

$$C_1 = 0.5, \quad C_2 = 0.6 \tag{48}$$

and an *overdamped case* with

$$C_1 = 0.5, \quad C_2 = 0.04. \tag{49}$$

Since C_1 and C_2 depend on the PLL parameters K_p and K_i as in (5), one can implement cases (48) and (49) under given voltage conditions by tuning the PLL.

Below we demonstrate how goals 1–3 listed in Sect. 2.6 may be reached using numerical integration of the autonomous comparison systems. Then we apply Theorem 2 to attain goal 4.

4.2.1 Estimation of the lock-in domain

Let us start with unbalance $\kappa = 10\%$. This case is shown in the left column of Fig. 4. Similarly to the proof of Theorem 1, the left comparison system oscillates around the pair of points $A_\pm = (0, \zeta_\pm)$. There is a stable limit cycle surrounding these points which is easily found by the numerical simulation of the left comparison system. The set $\mathcal{E}$ bounded by the limit cycle is shown in green – it is a forward invariant set of the PLL due to Proposition 1. The PLL has exactly one steady oscillation inside $\mathcal{E}$ because $\mathcal{E}$ satisfies condition (34) of Theorem 1, and the oscillation is attractive, at least within $\mathcal{E}$.

In order to construct an inner estimation of the lock-in domain, we compute the stable separatrices of the left comparison system that approach the points $B_\pm = (\pi, \zeta_\pm)$. Appendix B describes how the separatrices are approximated numerically via integration of the system in reverse time. The separatrices bound the blue region $\mathcal{D}$ which is a forward invariant set of the PLL since the boundary of $\mathcal{D}$ is crossed inward. Moreover, left comparison trajectories in $\mathcal{D}$ converge to $\mathcal{E}$ which easily implies that the PLL trajectories also converge to $\mathcal{E}$ and therefore to the steady oscillation inside $\mathcal{E}$. Thus, $\mathcal{D}$ is an inner estimation of the lock-in domain.

Finally, we compute the stable separatrices of the *right* comparison system approaching $B_\pm$. These are shown in red and are crossed by the PLL trajectories in the direction away from $\mathcal{D}$. Therefore, PLL trajectories starting from the red region marked $\mathcal{S}$ will make *at least* one crossing with the line $\beta = \pm\pi$ before *possibly* converging to the steady oscillation inside $\mathcal{E}$. It means that the lock-in domain cannot overlap with $\mathcal{S}$. Thus, the separatrices of the right comparison system outline an outer estimation of the lock-in domain.

The case of higher unbalance $\kappa = 15\%$ is shown in the right column of Fig. 4. One of the separatrices defining the set $\mathcal{D}$ does not wrap all the way around the phase cylinder, so $\mathcal{D}$ is bounded by only this one separatrix. Otherwise, everything else holds.

The higher the unbalance factor κ, the larger the set $\mathcal{E}$ becomes. Eventually it fails to satisfy condition (34). Then Theorem 1 still says that there is *at least one* steady oscillation inside $\mathcal{E}$ but cannot guarantee its uniqueness. For even higher unbalance, the limit cycle bounding $\mathcal{E}$ may cease to exist. It means that the technique of autonomous comparison systems is not applicable at this level of unbalance.

4.2.2 Comparison to the simulation

In Fig. 5 we compare the estimations of Fig. 4 to the numerical simulation results. The steady oscillation $\mathcal{O}_1$ near the origin is found easily by means of numerical simulation since it is stable. Then, we numerically solve the PLL system (4) starting from a grid of initial points and initial times and observe how they converge to $\mathcal{O}_1$. If they converge without crossing the line $\beta = \pm\pi$ then we assume that the initial point belongs to the lock-in domain and color it blue. If the solution crosses $\beta = \pm\pi$ one or more times but still converges to $\mathcal{O}_1$, we color the initial point a shade of red, similarly to how the red regions are colored in the balanced case (Fig. 1). If the trajectory fails to converge to $\mathcal{O}_1$ during the simulation time, we leave the initial point white.

To complete the picture, we also draw the unstable (saddle-type) oscillation $\mathcal{O}_1'$ near the point $(\pm\pi, 0)$ which is born from the saddle equilibrium of the balanced PLL [12, Lemma 4.5.1]. The oscillation and its separatrices lie between the separatrices of the left and right comparison systems – this statement is our analogue of [4, Theorem 7.1]. Since $\mathcal{O}_1'$ is unstable, we find it via numerical minimization of the distance between the initial point and its Poincaré image after one period.
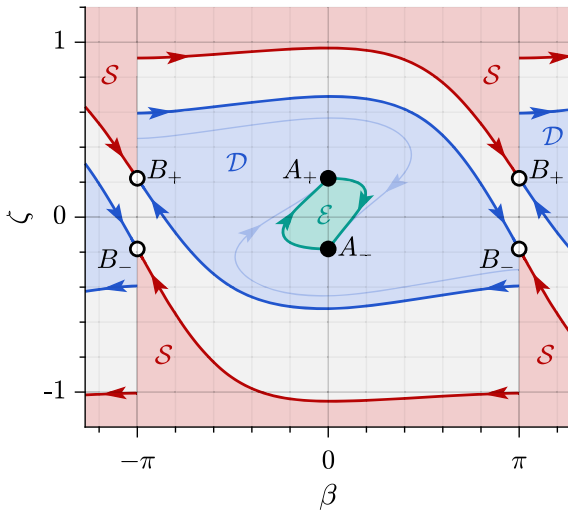
In some cases there appears to exist another unstable periodic solution $\mathcal{O}_2$ – a steady oscillation of the *second kind*, i.e., one that encircles the phase cylin-
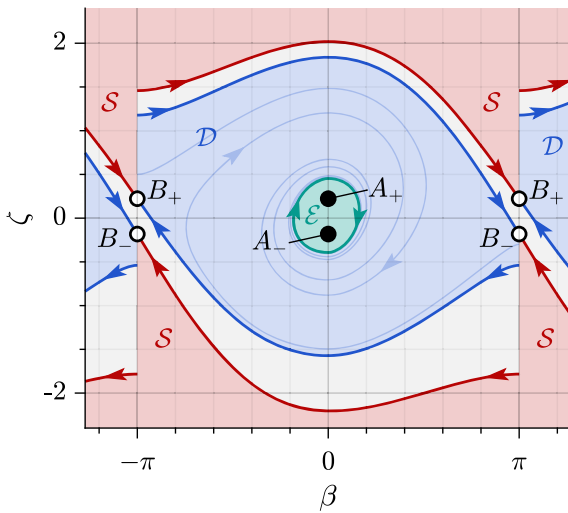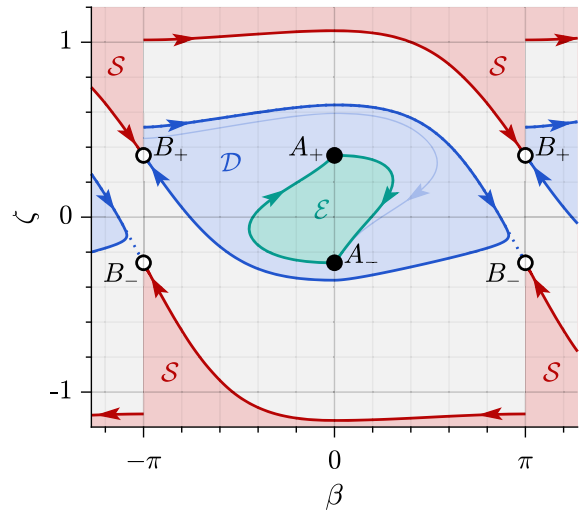
(a) Oscillatory case, $\kappa = 10\%$.
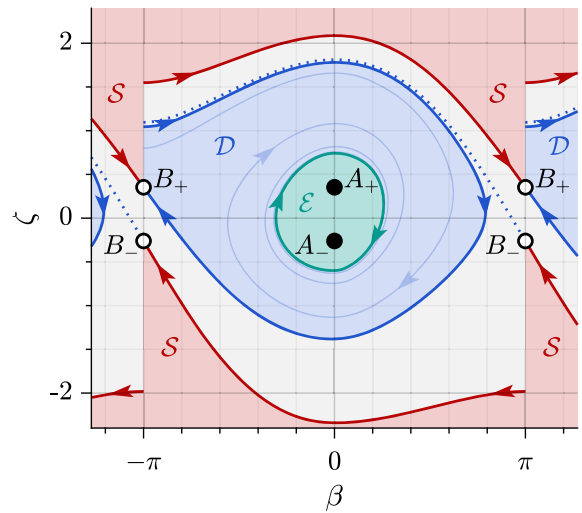
(b) Oscillatory case, $\kappa = 15\%$.

(c) Overdamped case, $\kappa = 10\%$.

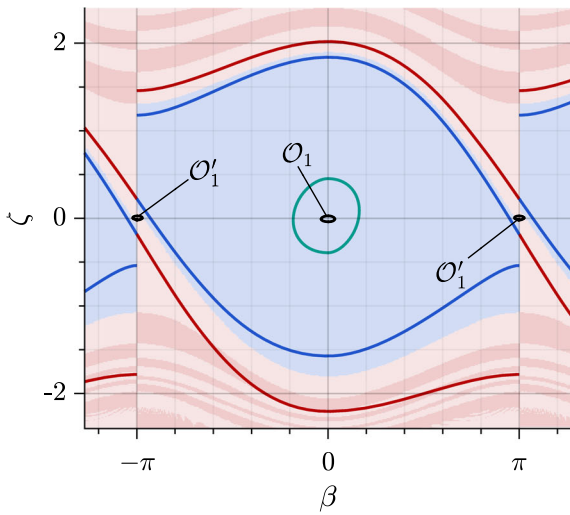(d) Overdamped case, $\kappa = 15\%$.

Fig. 4 Estimation of the steady oscillation near $(0, 0)$ and the lock-in domain of the unbalanced PLL (4). The steady oscillation is contained in the green region $\mathcal{E}$. The lock-in domain contains the blue region $\mathcal{D}$ and does not intersect with the red region $\mathcal{S}$.

The boundaries of $\mathcal{D}$ and $\mathcal{E}$ are formed by the trajectories of the left comparison system (16). The boundary of $\mathcal{S}$ – by the right comparison system (17)

der. Although unstable, $\mathcal{O}_2$ can still slow down the PLL's convergence to $\mathcal{O}_1$, as evident from the "condensation" of the red bands around $\mathcal{O}_2$ in Fig. 5. However, this oscillation always occurs around the line $\zeta = -2$ which makes it easily avoidable in practice. Indeed, since ζ is a *relative* frequency error, $\mathcal{O}_2$ corresponds to the frequency estimation oscillating around $-\omega$ instead

of ω. In practice, the PLL algorithm can be equipped with saturation that enforces the positiveness of the frequency estimation. This eliminates the whole region $\zeta \leq -1$ including the oscillation $\mathcal{O}_2$.
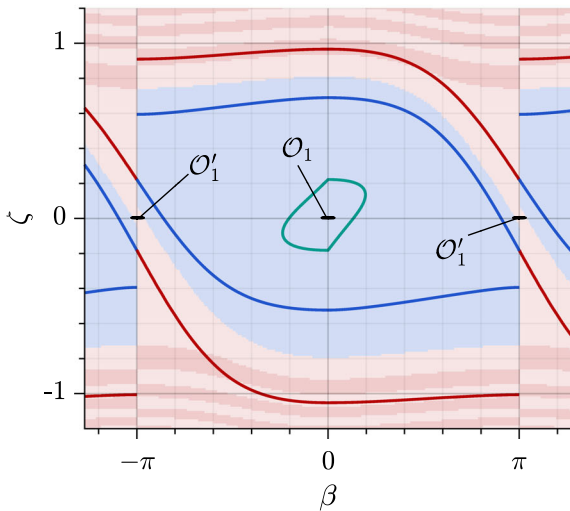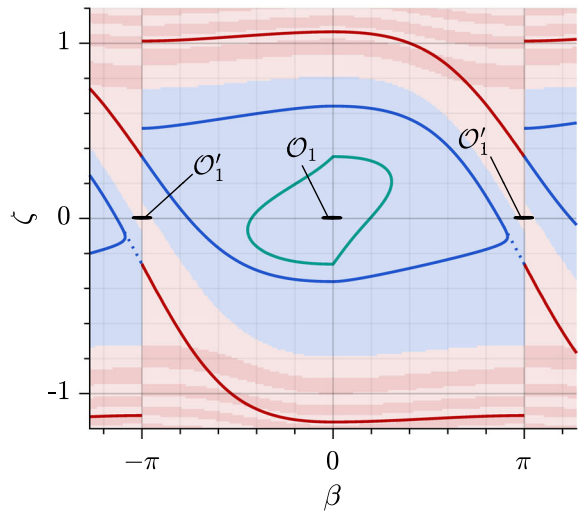
On the same practical note, in power grid applications the main frequency ω is known to be in a neighborhood of the nominal value (50 or 60 Hz). Thus, ζ

(a) Oscillatory case, $\kappa = 10\%$.
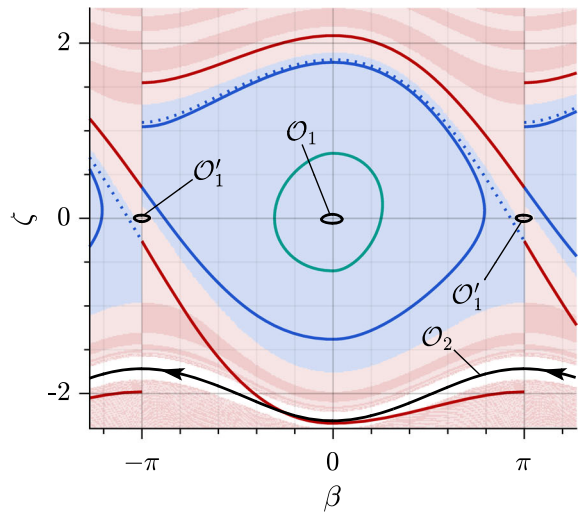
(b) Oscillatory case, $\kappa = 15\%$.

(c) Overdamped case, $\kappa = 10\%$.

(d) Overdamped case, $\kappa = 15\%$.

Fig. 5 Results of the simulation of unbalanced PLL (4) starting from various initial states. Initial points are colored depending on how many times the corresponding trajectory crosses the line $\beta = \pm\pi$ before converging to the steady oscillation $\mathcal{O}_1$. For the blue points, there are no crossings, independent of the initial time – such points belong to the lock-in domain. Red points can result in one or more crossings; they are colored a shade of red similarly to the red regions in Fig. 1 (balanced case). Points that did not clearly converge during the time of simulation are left white. Colored curves are the estimations of the lock-in domain from Fig. 4. $\mathcal{O}_1'$ is an unstable oscillation near the counterphase ($\beta = \pm\pi$). $\mathcal{O}_2$ is an unstable oscillation of the second kind

can be limited to a narrow range around zero. Furthermore, the value of the unbalance factor κ in normal operation rarely exceeds 2% [21]. For these values of unbalance and with ζ in a neighborhood of zero, our results indicate that the lock-in domain *provably* covers a major portion of the range of phase angles β.
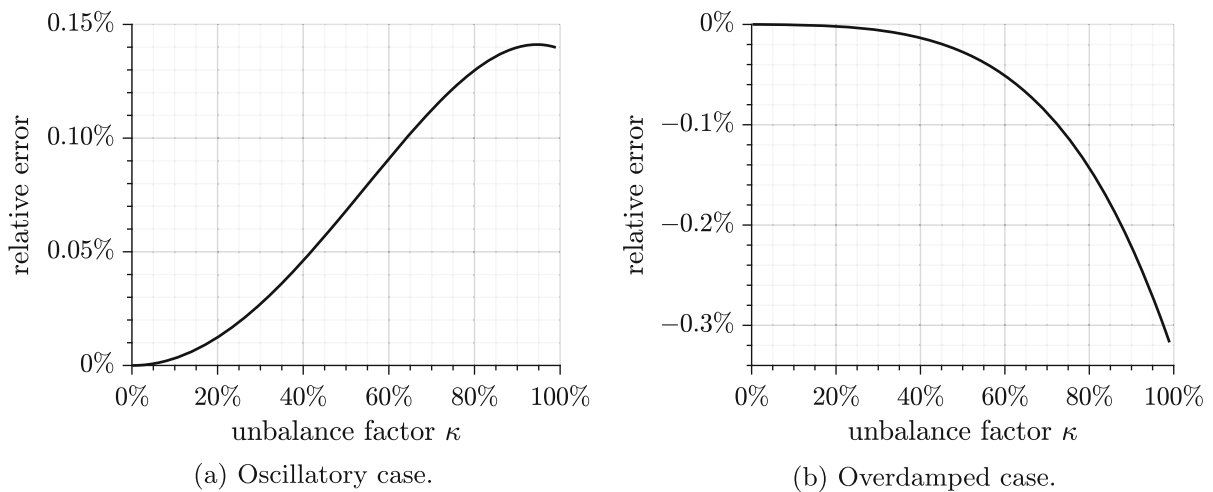
Fig. 6 Relative error (51) of the approximate time average of the phase error given by Theorem 2

4.2.3 Time average of the oscillation

In relation to goal 4 of Sect. 2.6, let us compare the time average of the dynamical phase error β in the steady oscillation to its approximation by Theorem 2. We compute the oscillation numerically for different values of κ and find the time average $\overline{\beta}$ via numerical integration. Theorem 2 gives the approximation

$$\overline{\beta} \approx \overline{\beta}_2 \kappa^2 \tag{50}$$

with the relative error

$$\frac{\overline{\beta}_2 \kappa^2 - \overline{\beta}}{\overline{\beta}} \tag{51}$$

which is shown in Fig. 6. We conclude that for the given sets of oscillatory and overdamped PLL parameters Theorem 2 provides a good estimation of $\overline{\beta}$.

5 Conclusion

We describe a nonlinear approach to the analysis of SRF-PLL under unbalanced voltage conditions. The following features are apparent:

1. The method is suitable for higher unbalance compared to the linearization technique.
2. It shows the existence of a unique steady oscillation whose lock-in domain covers a relatively wide range of phases. Assuming that the AC grid is operating under normal conditions (i.e., close to the nominal frequency and close to balance), the results prove that the lock-in range of phase angles is close to $(-\pi, \pi)$. Under given conditions, the analysis can be used to assess if SRF-PLL is sufficiently reliable.
3. The nonlinear approach yields an approximation of the time average of the PLL's phase error which turns out to be a second-order quantity with respect to the unbalance factor.

Future work may include:

1. Application of the method of autonomous comparison systems to other PLL types and operating conditions (e.g., with voltage harmonics).
2. After the κ and κ^2 Taylor terms of the steady oscillation are determined like in the proof of Theorem 2, the residual term can be estimated via the comparison theory applied to its equation (47). In this way, we can improve the set $\mathcal{E}$ where the steady oscillation is localized.
3. Instead of approximating the time-periodic system (4) by autonomous comparison systems, one can take another step and use even rougher approximations to allow analytical estimations, rather than numerical. For example, one approach is based on piecewise linear comparison systems [18] and another employs collocation-based approximations [13].

4. As the proportion of renewable energy resources in the power grid is rising, it becomes crucial to understand the interaction between grid-tied PLL-based voltage inverters and the grid itself. In this paper we considered the PLL dynamics in isolation, but the same method may be helpful in the analysis of one or multiple inverters in closed loop with the grid.

Declarations

Appendix A Derivation of SRF-PLL dynamics

Consider the three-phase voltage

$$\boldsymbol{v} = \begin{bmatrix} v_a \\ v_b \\ v_c \end{bmatrix} = \begin{bmatrix} V_a \cos(\omega t + \phi_a) \\ V_b \cos\left(\omega t + \phi_b - \frac{2\pi}{3}\right) \\ V_c \cos\left(\omega t + \phi_c + \frac{2\pi}{3}\right) \end{bmatrix}. \tag{A1}$$

Assumption 1 The frequency ω, peak voltages V_a, V_b, V_c, and phase angles ϕ_a, ϕ_b, ϕ_c are all constant.

Definition 5 Voltage (A1) is called *balanced* if $V_a = V_b = V_c$ and $\phi_a = \phi_b = \phi_c$. Otherwise it is called *unbalanced*.

In the balanced case, the task of the PLL is to determine the phase $\omega t + \phi_a$ of the first voltage component. As for the unbalanced conditions, the meaning of phase estimation will be specified in Sect. A.2.

A.1 Park's Transformation

In the following, we use the standard definition of the Park transform where we omit the last ("zero") component and consider only the direct and quadrature components. This truncated version is also known as the *dq* transform.

Definition 6 [23, Appendix C] Given an arbitrary angle ϕ, *Park's transformation* of the voltage (A1) is

$$\begin{bmatrix} v_d \\ v_q \end{bmatrix} = \frac{2}{3} \begin{bmatrix} \cos\phi & \cos\left(\phi - \frac{2\pi}{3}\right) & \cos\left(\phi + \frac{2\pi}{3}\right) \\ -\sin\phi & -\sin\left(\phi - \frac{2\pi}{3}\right) & -\sin\left(\phi + \frac{2\pi}{3}\right) \end{bmatrix} \boldsymbol{v} \tag{A2}$$

where v_d and v_q are called the *direct* and *quadrature* components, respectively.

For convenience, we rewrite the Park transform using Fortescue's symmetrical component theory [10]. First, define the phasor

$$\boldsymbol{\Phi} = \begin{bmatrix} V_a \, \mathrm{e}^{j\phi_a} \\ V_b \, \mathrm{e}^{j(-2\pi/3+\phi_b)} \\ V_c \, \mathrm{e}^{j(2\pi/3+\phi_c)} \end{bmatrix} \in \mathbb{C}^3 \tag{A3}$$

where j is the imaginary unit. Voltage (A1) is expressed as

$$\boldsymbol{v} = \tfrac{1}{2}\boldsymbol{\Phi}\mathrm{e}^{j\omega t} + \tfrac{1}{2}\overline{\boldsymbol{\Phi}}\mathrm{e}^{-j\omega t} \tag{A4}$$

where $\overline{\boldsymbol{\Phi}}$ is the complex conjugate of $\boldsymbol{\Phi}$. We shall treat the phasor space $\mathbb{C}^3$ as a 3-dimensional Hilbert space over $\mathbb{C}$ with the inner product

$$\langle \boldsymbol{\Phi}, \boldsymbol{\Psi} \rangle := \boldsymbol{\Phi}^* \boldsymbol{\Psi} \tag{A5}$$

where $\boldsymbol{\Phi}^*$ is the conjugate transpose of $\boldsymbol{\Phi}$. Note that we use the "physical" convention for the inner product definition, i.e., linear in the *second* argument.

Fortescue's symmetrical components are then as follows.

Definition 7 [17, Section 9.2] *Positive, negative, and zero sequence components* (Φ_p, Φ_n, and Φ_0, respectively) *of the phasor* $\boldsymbol{\Phi}$ *are*

$$\Phi_i = \tfrac{1}{3}\langle e_i, \boldsymbol{\Phi}\rangle \in \mathbb{C}, \quad i \in \{p, n, 0\} \tag{A6a}$$

where

$$\boldsymbol{e}_p = \begin{bmatrix} 1 \\ e^{-j2\pi/3} \\ e^{j2\pi/3} \end{bmatrix}, \quad \boldsymbol{e}_n = \begin{bmatrix} 1 \\ e^{j2\pi/3} \\ e^{-j2\pi/3} \end{bmatrix}, \quad \boldsymbol{e}_0 = \begin{bmatrix} 1 \\ 1 \\ 1 \end{bmatrix}. \tag{A6b}$$

Park's transform can be formulated more compactly as

$$v_d + jv_q = \tfrac{2}{3}e^{-j\phi}\langle e_p, \boldsymbol{v}\rangle, \quad v_d, v_q \in \mathbb{R}. \tag{A7}$$

Combining this with (A4) and noticing that $\bar{\boldsymbol{e}}_p = \boldsymbol{e}_n$ we come to the following conclusion.

Proposition 2 *Park's direct and quadrature components* v_d *and* v_q *can be determined from the equation*

$$v_d + jv_q = e^{-j\phi}\big(\Phi_p e^{j\omega t} + \overline{\Phi}_n e^{-j\omega t}\big), \quad v_d, v_q \in \mathbb{R} \tag{A8}$$

where Φ_p *and* Φ_n *are, respectively, the positive and negative sequence components of the voltage phasor.*

A.2 Phase-locked loop

The task of the phase-locked loop is to track the phase of the *positive sequence* voltage which equals $\arg \Phi_p + \omega t$. This motivates the following definition.

Definition 8 Angle ϕ of Park's transform (A8) is said to be *phase-locked* to the voltage (A1) if $\phi \equiv \arg \Phi_p + \omega t \pmod{2\pi}$.

In the balanced case $\Phi_n = 0$, and due to (A8) the phase lock implies $v_q = 0$. Because of this, the PLL algorithm assumes $v_q = 0$ as its objective and manipulates the angle ϕ to stabilize v_q to zero. Most commonly, stabilization is achieved by a PI (proportional-integral) controller. The corresponding PLL equations are

$$\dot{\phi} = K_p v_q + z + \omega_{\text{nom}}, \tag{A9a}$$
$$\dot{z} = K_i v_q \tag{A9b}$$

where z is the integrator state, ω_{nom} is the nominal voltage frequency, $K_p > 0$ is the *proportional gain*, and $K_i > 0$ is the *integral gain* of the PI controller.

If phase lock is achieved, ϕ becomes the positive sequence phase and $z + \omega_{\text{nom}}$ the frequency of the grid.

In order to put (A9) into a more convenient form, we introduce new notation: the *phase locking error*

$$\widetilde{\phi} = \phi - (\arg \Phi_p + \omega t) \tag{A10}$$

and the following common definition.

Definition 9 The *unbalance factor* of the voltage (A1) is

$$\kappa = \frac{|\Phi_n|}{|\Phi_p|}. \tag{A11}$$

Remark 9 This definition of unbalance, also known as *true unbalance*, is adopted, e.g., by IEEE [15] and IEC [14].

Assumption 2 $0\% \leq \kappa < 100\%$.

Remark 10 Under normal conditions κ rarely exceeds 2% – the so-called "compatibility level" [21]. Stronger unbalance may occur during temporary unsymmetrical faults.

From (A8) we obtain

$$v_d + jv_q = |\Phi_p|e^{-j\widetilde{\phi}}\big(1 + \kappa e^{-j2\omega(t+\triangle t)}\big) \tag{A12a}$$

where

$$\triangle t = \frac{\arg \Phi_p + \arg \Phi_n}{2\omega}. \tag{A12b}$$

Assuming the exponential representation

$$1 + \kappa e^{-j\psi} = \mu(\psi)e^{-j\alpha(\psi)}, \quad \mu(\psi), \alpha(\psi) \in \mathbb{R}$$

$$(A13)$$

we have

$$v_d + j v_q = |\Phi_p| \mu\big(2\omega(t + \triangle t)\big) e^{-j(\widetilde{\phi} + \alpha(2\omega(t + \triangle t)))}.$$
$$(A14)$$

Remark 11 Functions $\mu(\cdot)$ and $\alpha(\cdot)$ are 2π-periodic. In the balanced case $\mu(\cdot) = 1$ and $\alpha(\cdot) = 0$.

Assumption 3 $\triangle t = 0$.

Remark 12 Time $\triangle t$ is the forward time shift inside the PLL relative to the voltage oscillation. It effects the time shift of the phase locking error. For the purposes of qualitative analysis it is safe to ignore the time shift, hence Assumption 3 is made.

Let us introduce new coordinates

$$\delta(t) = \widetilde{\phi}(t) + \alpha(2\omega t), \qquad (A15a)$$
$$\gamma(t) = z(t) + \omega_{\text{nom}} - \omega. \qquad (A15b)$$

System (A9) turns into

$$\dot{\delta} = -K_p |\Phi_p| \mu(2\omega t) \sin \delta + \gamma + 2\omega\alpha'(2\omega t),$$
$$(A16a)$$
$$\dot{\gamma} = -K_i |\Phi_p| \mu(2\omega t) \sin \delta. \qquad (A16b)$$

Relation (A13) gives

$$\mu(\psi) = \sqrt{1 + 2\kappa \cos \psi + \kappa^2}, \qquad (A17a)$$
$$2\alpha'(\psi) = \frac{2\kappa \cos \psi + 2\kappa^2}{1 + 2\kappa \cos \psi + \kappa^2} = F\big(\mu(\psi)\big) \qquad (A17b)$$

where

$$F(\mu) = 1 - \frac{1 - \kappa^2}{\mu^2}. \qquad (A17c)$$

Therefore, (A16) can be rewritten as

$$\dot{\delta} = -K_1 \mu(2\omega t) \sin \delta + \gamma + \omega F\big(\mu(2\omega t)\big), \quad (A18a)$$
$$\dot{\gamma} = -K_2 \mu(2\omega t) \sin \delta \qquad (A18b)$$

where

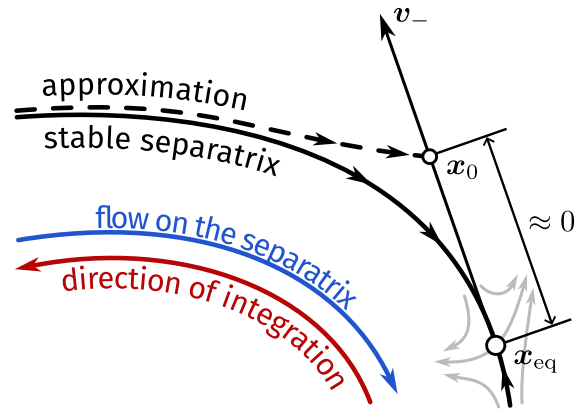$$K_1 = K_p |\Phi_p|, \quad K_2 = K_i |\Phi_p|. \qquad (A18c)$$

Fig. 7 Approximation of the stable separatrix approaching the saddle equilibrium x_{eq} via reverse-time integration of the system. The initial point x_0 is chosen close to x_{eq} along the eigenvector v_- which corresponds to the negative eigenvalue at x_{eq}

We arrive at the following.

Proposition 3 *Under Assumptions 1–3 the SRF-PLL equations can be written in the form* (A18). *The phase locking error is*

$$\widetilde{\phi} = \delta - \alpha(2\omega t). \qquad (A19)$$

If Assumption 3 does not hold, $\widetilde{\phi}$ experiences a forward time shift $\triangle t$ given in (A12b).

In the language of system theory, Proposition 3 describes a system where the signals $\mu(2\omega t)$ and $\alpha(2\omega t)$ are inputs, and the phase error $\widetilde{\phi}$ is the output. The output $\widetilde{\phi}$ contains two parts: the *dynamical* part δ produced by the nonlinear filter (A18), and the *passthrough* part, i.e., the input $\alpha(2\omega t)$ going directly to the output. The latter part is simply a $\frac{\pi}{\omega}$-periodic function, easy to calculate and analyze. Hence, in this paper we look closer at the term δ and give it a special name.

Definition 10 The angle δ produced by the PLL dynamics (A18) is called the *dynamical phase error*.

Appendix B Computation of separatrices

Consider a system

$$\dot{x} = f(x), \quad x \in \mathbb{R}^2. \qquad (B20)$$

Suppose x_{eq} is a saddle equilibrium, i.e., the matrix of the linear approximation of $f(x)$ at x_{eq} has one positive and one negative eigenvalue. Stable separatrices are two trajectories that approach x_{eq} from the directions $\pm v_-$ where v_- is an eigenvector corresponding to the negative eigenvalue. Figure 7 illustrates a common approach to finding the stable separatrix via numerical integration. One picks a point x_0 close to x_{eq} in the direction of v_- (or $-v_-$) and integrates the system starting from x_0 *in reverse time*. As the stable separatrix at the saddle point is itself an *unstable manifold*, at least near x_{eq}, in reverse time it becomes stable and attracts the trajectory starting from x_0.

In the context of Sect. 4.2.1, we need to compute the stable separatrices of the comparison systems approaching points B_+ and B_-. For example, consider the separatrix of the left comparison system that tends to B_+ (coordinates $(-\pi, \zeta_+)$) from the right. To the right of B_+, the left comparison system has the linearization matrix

$$\begin{bmatrix} C_1 & \frac{1}{1-\kappa} \\ C_2 & 0 \end{bmatrix} \tag{B21}$$

with a negative eigenvalue

$$\lambda_- = \frac{1}{2}\left(C_1 - \sqrt{C_1^2 + \frac{4C_2}{1-\kappa}} \right) \tag{B22}$$

and the corresponding eigenvector

$$-\begin{bmatrix} \lambda_- \\ C_2 \end{bmatrix} \tag{B23}$$

pointing to the right and downward. To approximate the separatrix, we start from the point

$$x_0 = \begin{bmatrix} -\pi \\ \zeta_+ \end{bmatrix} - \varepsilon \begin{bmatrix} \lambda_- \\ C_2 \end{bmatrix} \tag{B24}$$

with a small $\varepsilon > 0$ and integrate the left comparison system numerically in reverse time. Other separatrices are approximated likewise.

References

1. Ali, Z., Christofides, N., Hadjidemetriou, L., Kyriakides, E., Yang, Y., Blaabjerg, F.: Three-phase phase-locked loop synchronization algorithms for grid-connected renewable energy systems: a review. Renew. Sustain. Energy Rev. **90**, 434–452 (2018). https://doi.org/10.1016/j.rser.2018.03.086

2. Amato, F.: Robust control of linear systems subject to uncertain time-varying parameters. Springer, Heidelberg (2006)

3. Angeli, D.: A Lyapunov approach to incremental stability properties. IEEE Trans. Autom. Control **47**(3), 410–421 (2002). https://doi.org/10.1109/9.989067

4. Belykh, V.N.: The qualitative investigation of a second order nonautonomous nonlinear equation. Differ. Uravn. **11**(10), 1738–1753 (1975). (**in Russian**)

5. Best, R.E.: Phase-Locked Loops: Design, Simulation, and Applications, 6th edn. McGraw-Hill, New York (2007)

6. Bravo, M., Garcés, A.,Montoya, O.D., Baier, C.R.: Nonlinear analysis for the three-phase PLL: a new look for a classical problem. In 2018 IEEE 19th Workshop on Control and Modeling for Power Electronics (COMPEL), pp. 1–6

7. Chung, S.-K.: A phase tracking system for three phase utility interface inverters. IEEE Trans. Power Electron. **15**(3), 431–438 (2000). https://doi.org/10.1109/63.844502

8. D'Humières, D., Beasley, M.R., Huberman, B.A., Libchaber, A.: Chaotic states and routes to chaos in the forced pendulum. Phys. Rev. A **26**(6), 3483–3496 (1982). https://doi.org/10.1103/PhysRevA.26.3483

9. Escobar, G., Ibarra, L., Valdez-Resendiz, J.E., Mayo-Maldonado, J.C., Guillen, D.: Nonlinear stability analysis of the conventional SRF-PLL and enhanced SRF-EPLL. IEEE Access **9**, 59446–59455 (2021). https://doi.org/10.1109/ACCESS.2021.3073063

10. Fortescue, C.L.: Method of symmetrical co-ordinates applied to the solution of polyphase networks. Trans. Am. Inst. Electr. Eng. XXXVI **I**(2), 1027–1140 (1918). https://doi.org/10.1109/T-AIEE.1918.4765570

11. Fromion, V., Scorletti, G.: Connecting nonlinear incremental Lyapunov stability with the linearizations Lyapunov stability. In 44th IEEE Conference on Decision and Control (CDC), pp. 4736–4741. (2005). https://doi.org/10.1109/CDC.2005.1582910

12. Guckenheimer, J., Holmes, P.: Nonlinear oscillations, dynamical systems, and bifurcations of vector fields, volume 42 of Applied Mathematical Sciences. Springer, New York, NY, (1983). https://doi.org/10.1007/978-1-4612-1140-2

13. Harb, B.A., Al-Ajlouni, A.F.: A collocation-based algorithm for computing the pull-in range of a class of phase-locked loops. Nonlinear Dyn. **35**(3), 249–258 (2004). https://doi.org/10.1023/B:NODY.0000027911.21375.5a

14. IEC Standard 60034-26:2006: Rotating electrical machines—Part 26: effects of unbalanced voltages on the performance of three-phase cage induction motors

15. IEEE Standard 1159-2019: Recommended practice for monitoring electric power quality. https://doi.org/10.1109/IEEESTD.2016.7553421

16. Indeitsev, D.A., Belyaev, Y.V., Lukin, A.V., Popov, I.A.: Nonlinear dynamics of MEMS resonator in PLL-AGC self-oscillation loop. Nonlinear Dyn. **104**(4), 3187–3204 (2021). https://doi.org/10.1007/s11071-021-06586-x

17. Krause, P.C., Wasynczuk, O., Sudhoff, S.D., Pekarek, S.: Analysis of Electric Machinery and Drive Systems, 3rd edn. Wiley, Hoboken (2013)

18. Kuznetsov, N.V., Lobachev, M.Y., Yuldashev, M.V., Yuldashev, R.V., Tavazoei, M.S.: The Gardner problem on the

lock-in range of second-order type 2 phase-locked loops. IEEE Trans. Autom. Control **68**(12), 7436–7450 (2023). https://doi.org/10.1109/TAC.2023.3277896

19. Leonov, G.A., Kuznetsov, N.V., Yuldashev, M.V., Yuldashev, R.V.: Hold-in, pull-in, and lock-in ranges of PLL circuits: rigorous mathematical definitions and limitations of classical theory. IEEE Trans. Circuits Syst. I Regul. Pap. **62**(10), 2454–2464 (2015). https://doi.org/10.1109/TCSI.2015.2476295

20. Leonov, G.A., Reitmann, V., Smirnova, V.B.: Nonlocal Methods for Pendulum-like Feedback Systems. Vieweg+Teubner, Landesmuseum (1992)

21. Moller, F., Meyer, J.: Survey of voltage unbalance and unbalanced power in German public LV networks. In 20th International Conference on Harmonics & Quality of Power (ICHQP), pp. 1–6. (2022). https://doi.org/10.1109/ICHQP53011.2022.9808568

22. Ortega, A., Milano, F.: Frequency control of distributed energy resources in distribution networks. IFAC-PapersOnLine **51**(28), 37–42 (2018). https://doi.org/10.1016/j.ifacol.2018.11.674

23. Umans, S.D., Fitzgerald, A.E.: Fitzgerald & Kingsley's electric machinery, 7th edn. McGraw-Hill, New York City (2014)

24. Yoshizawa, T.: Stability Theory and the Existence of Periodic Solutions and Almost Periodic Solutions. Springer, New York (1975)